View metadata, citation and similar papers at core.ac.uk
brought to you by CORE
provided by UNT Digital Library

arXiv:0705.4629v2 [hep-ex] 4 Oct 2007

Measurement of Transverse Single-Spin Asymmetries for Di-Jet Production in Proton-Proton Collisions at $\sqrt{s} = 200$ GeV

B.I. Abelev,[9] M.M. Aggarwal,[30] Z. Ahammed,[45] B.D. Anderson,[20] D. Arkhipkin,[13] G.S. Averichev,[12] Y. Bai,[28] J. Balewski,[17] O. Barannikova,[9] L.S. Barnby,[2] J. Baudot,[18] S. Baumgart,[50] V.V. Belaga,[12] A. Bellingeri-Laurikainen,[40] R. Bellwied,[48] F. Benedosso,[28] R.R. Betts,[9] S. Bhardwaj,[35] A. Bhasin,[19] A.K. Bhati,[30] H. Bichsel,[47] J. Bielcik,[50] J. Bielcikova,[50] L.C. Bland,[3] S-L. Blyth,[22] M. Bombara,[2] B.E. Bonner,[36] M. Botje,[28] J. Bouchet,[40] A.V. Brandin,[26] T.P. Burton,[2] M. Bystersky,[11] X.Z. Cai,[39] H. Caines,[50] M. Calderón de la Barca Sánchez,[6] J. Callner,[9] O. Catu,[50] D. Cebra,[6] M.C. Cervantes,[41] Z. Chajecki,[29] P. Chaloupka,[11] S. Chattopadhyay,[45] H.F. Chen,[38] J.H. Chen,[39] J.Y. Chen,[49] J. Cheng,[43] M. Cherney,[10] A. Chikanian,[50] W. Christie,[3] S.U. Chung,[3] R.F. Clarke,[41] M.J.M. Codrington,[41] J.P. Coffin,[18] T.M. Cormier,[48] M.R. Cosentino,[37] J.G. Cramer,[47] H.J. Crawford,[5] D. Das,[45] S. Dash,[15] M. Daugherity,[42] M.M. de Moura,[37] T.G. Dedovich,[12] M. DePhillips,[3] A.A. Derevschikov,[32] L. Didenko,[3] T. Dietel,[14] P. Djawotho,[17] S.M. Dogra,[19] X. Dong,[22] J.L. Drachenberg,[41] J.E. Draper,[6] F. Du,[50] V.B. Dunin,[12] J.C. Dunlop,[3] M.R. Dutta Mazumdar,[45] W.R. Edwards,[22] L.G. Efimov,[12] V. Emelianov,[26] J. Engelage,[5] G. Eppley,[36] B. Erazmus,[40] M. Estienne,[18] P. Fachini,[3] R. Fatemi,[23] J. Fedorisin,[12] A. Feng,[49] P. Filip,[13] E. Finch,[50] V. Fine,[3] Y. Fisyak,[3] J. Fu,[49] C.A. Gagliardi,[41] L. Gaillard,[2] M.S. Ganti,[45] E. Garcia-Solis,[9] V. Ghazikhanian,[7] P. Ghosh,[45] Y.N. Gorbunov,[10] H. Gos,[46] O. Grebenyuk,[28] D. Grosnick,[44] B. Grube,[34] S.M. Guertin,[7] K.S.F.F. Guimaraes,[37] A. Gupta,[19] N. Gupta,[19] B. Haag,[6] T.J. Hallman,[3] A. Hamed,[41] J.W. Harris,[50] W. He,[17] M. Heinz,[50] T.W. Henry,[41] S. Heppelmann,[31] B. Hippolyte,[18] A. Hirsch,[33] E. Hjort,[22] A.M. Hoffman,[23] G.W. Hoffmann,[42] D.J. Hofman,[9] R.S. Hollis,[9] M.J. Horner,[22] H.Z. Huang,[7] E.W. Hughes,[4] T.J. Humanic,[29] G. Igo,[7] A. Iordanova,[9] P. Jacobs,[22] W.W. Jacobs,[17] P. Jakl,[11] P.G. Jones,[2] E.G. Judd,[5] S. Kabana,[40] K. Kang,[43] J. Kapitan,[11] M. Kaplan,[8] D. Keane,[20] A. Kechechyan,[12] D. Kettler,[47] V.Yu. Khodyrev,[32] J. Kiryluk,[22] A. Kisiel,[29] E.M. Kislov,[12] S.R. Klein,[22] A.G. Knospe,[50] A. Kocoloski,[23] D.D. Koetke,[44] T. Kollegger,[14] M. Kopytine,[20] L. Kotchenda,[26] V. Kouchpil,[11] K.L. Kowalik,[22] P. Kravtsov,[26] V.I. Kravtsov,[32] K. Krueger,[1] C. Kuhn,[18] A.I. Kulikov,[12] A. Kumar,[30] P. Kurnadi,[7] A.A. Kuznetsov,[12] M.A.C. Lamont,[50] J.M. Landgraf,[3] S. Lange,[14] S. LaPointe,[48] F. Laue,[3] J. Lauret,[3] A. Lebedev,[3] R. Lednicky,[13] C-H. Lee,[34] S. Lehocka,[12] M.J. LeVine,[3] C. Li,[38] Q. Li,[48] Y. Li,[43] G. Lin,[50] X. Lin,[49] S.J. Lindenbaum,[27] M.A. Lisa,[29] F. Liu,[49] H. Liu,[38] J. Liu,[36] L. Liu,[49] T. Ljubicic,[3] W.J. Llope,[36] R.S. Longacre,[3] W.A. Love,[3] Y. Lu,[49] T. Ludlam,[3] D. Lynn,[3] G.L. Ma,[39] J.G. Ma,[7] Y.G. Ma,[39] D.P. Mahapatra,[15] R. Majka,[50] L.K. Mangotra,[19] R. Manweiler,[44] S. Margetis,[20] C. Markert,[42] L. Martin,[40] H.S. Matis,[22] Yu.A. Matulenko,[32] T.S. McShane,[10] A. Meschanin,[32] J. Millane,[23] M.L. Miller,[23] N.G. Minaev,[32] S. Mioduszewski,[41] A. Mischke,[28] J. Mitchell,[36] B. Mohanty,[22] D.A. Morozov,[32] M.G. Munhoz,[37] B.K. Nandi,[16] C. Nattrass,[50] T.K. Nayak,[45] J.M. Nelson,[2] C. Nepali,[20] P.K. Netrakanti,[33] L.V. Nogach,[32] S.B. Nurushev,[32] G. Odyniec,[22] A. Ogawa,[3] V. Okorokov,[26] D. Olson,[22] M. Pachr,[11] S.K. Pal,[45] Y. Panebratsev,[12] A.I. Pavlinov,[48] T. Pawlak,[46] T. Peitzmann,[28] V. Perevoztchikov,[3] C. Perkins,[5] W. Peryt,[46] S.C. Phatak,[15] M. Planinic,[51] J. Pluta,[46] N. Poljak,[51] N. Porile,[33] A.M. Poskanzer,[22] M. Potekhin,[3] E. Potrebenikova,[12] B.V.K.S. Potukuchi,[19] D. Prindle,[47] C. Pruneau,[48] N.K. Pruthi,[30] J. Putschke,[22] I.A. Qattan,[17] R. Raniwala,[35] S. Raniwala,[35] R.L. Ray,[42] D. Relyea,[4] A. Ridiger,[26] H.G. Ritter,[22] J.B. Roberts,[36] O.V. Rogachevskiy,[12] J.L. Romero,[6] A. Rose,[22] C. Roy,[40] L. Ruan,[3] M.J. Russcher,[28] R. Sahoo,[15] I. Sakrejda,[22] T. Sakuma,[23] S. Salur,[50] J. Sandweiss,[50] M. Sarsour,[41] P.S. Sazhin,[12] J. Schambach,[42] R.P. Scharenberg,[33] N. Schmitz,[24] J. Seger,[10] I. Selyuzhenkov,[48] P. Seyboth,[24] A. Shabetai,[18] E. Shahaliev,[12] M. Shao,[38] M. Sharma,[30] W.Q. Shen,[39] S.S. Shimanskiy,[12] E.P. Sichtermann,[22] F. Simon,[23] R.N. Singaraju,[45] N. Smirnov,[50] R. Snellings,[28] P. Sorensen,[3] J. Sowinski,[17] J. Speltz,[18] H.M. Spinka,[1] B. Srivastava,[33] A. Stadnik,[12] T.D.S. Stanislaus,[44] D. Staszak,[7] J. Stevens,[17] R. Stock,[14] M. Strikhanov,[26] B. Stringfellow,[33] A.A.P. Suaide,[37] M.C. Suarez,[9] N.L. Subba,[20] M. Sumbera,[11] X.M. Sun,[22] Z. Sun,[21] B. Surrow,[23] T.J.M. Symons,[22] A. Szanto de Toledo,[37] J. Takahashi,[37] A.H. Tang,[3] T. Tarnowsky,[33] J.H. Thomas,[22] A.R. Timmins,[2] S. Timoshenko,[26] M. Tokarev,[12] T.A. Trainor,[47] S. Trentalange,[7] R.E. Tribble,[41] O.D. Tsai,[7] J. Ulery,[33] T. Ullrich,[3] D.G. Underwood,[1] G. Van Buren,[3] N. van der Kolk,[28] M. van Leeuwen,[22] A.M. Vander Molen,[25] R. Varma,[16] I.M. Vasilevski,[13] A.N. Vasiliev,[32] R. Vernet,[18] S.E. Vigdor,[17] Y.P. Viyogi,[15] S. Vokal,[12] S.A. Voloshin,[48] M. Wada,[10] W.T. Waggoner,[10] F. Wang,[33] G. Wang,[7] J.S. Wang,[21] X.L. Wang,[38] Y. Wang,[43] J.C. Webb,[44] G.D. Westfall,[25] C. Whitten Jr.,[7] H. Wieman,[22] S.W. Wissink,[17] R. Witt,[50] J. Wu,[38] Y. Wu,[49] N. Xu,[22] Q.H. Xu,[22] Z. Xu,[3] P. Yepes,[36] I-K. Yoo,[34]

Q. Yue,[43] V.I. Yurevich,[12] M. Zawisza,[46] W. Zhan,[21] H. Zhang,[3] W.M. Zhang,[20] Y. Zhang,[38] Z.P. Zhang,[38] Y. Zhao,[38] C. Zhong,[39] J. Zhou,[36] R. Zoulkarneev,[13] Y. Zoulkarneeva,[13] A.N. Zubarev,[12] and J.X. Zuo[39]

(STAR Collaboration)

[1] *Argonne National Laboratory, Argonne, Illinois 60439*
[2] *University of Birmingham, Birmingham, United Kingdom*
[3] *Brookhaven National Laboratory, Upton, New York 11973*
[4] *California Institute of Technology, Pasadena, California 91125*
[5] *University of California, Berkeley, California 94720*
[6] *University of California, Davis, California 95616*
[7] *University of California, Los Angeles, California 90095*
[8] *Carnegie Mellon University, Pittsburgh, Pennsylvania 15213*
[9] *University of Illinois at Chicago, Chicago, Illinois 60607*
[10] *Creighton University, Omaha, Nebraska 68178*
[11] *Nuclear Physics Institute AS CR, 250 68 Řež/Prague, Czech Republic*
[12] *Laboratory for High Energy (JINR), Dubna, Russia*
[13] *Particle Physics Laboratory (JINR), Dubna, Russia*
[14] *University of Frankfurt, Frankfurt, Germany*
[15] *Institute of Physics, Bhubaneswar 751005, India*
[16] *Indian Institute of Technology, Mumbai, India*
[17] *Indiana University, Bloomington, Indiana 47408*
[18] *Institut de Recherches Subatomiques, Strasbourg, France*
[19] *University of Jammu, Jammu 180001, India*
[20] *Kent State University, Kent, Ohio 44242*
[21] *Institute of Modern Physics, Lanzhou, China*
[22] *Lawrence Berkeley National Laboratory, Berkeley, California 94720*
[23] *Massachusetts Institute of Technology, Cambridge, MA 02139-4307*
[24] *Max-Planck-Institut für Physik, Munich, Germany*
[25] *Michigan State University, East Lansing, Michigan 48824*
[26] *Moscow Engineering Physics Institute, Moscow Russia*
[27] *City College of New York, New York City, New York 10031*
[28] *NIKHEF and Utrecht University, Amsterdam, The Netherlands*
[29] *Ohio State University, Columbus, Ohio 43210*
[30] *Panjab University, Chandigarh 160014, India*
[31] *Pennsylvania State University, University Park, Pennsylvania 16802*
[32] *Institute of High Energy Physics, Protvino, Russia*
[33] *Purdue University, West Lafayette, Indiana 47907*
[34] *Pusan National University, Pusan, Republic of Korea*
[35] *University of Rajasthan, Jaipur 302004, India*
[36] *Rice University, Houston, Texas 77251*
[37] *Universidade de Sao Paulo, Sao Paulo, Brazil*
[38] *University of Science & Technology of China, Hefei 230026, China*
[39] *Shanghai Institute of Applied Physics, Shanghai 201800, China*
[40] *SUBATECH, Nantes, France*
[41] *Texas A&M University, College Station, Texas 77843*
[42] *University of Texas, Austin, Texas 78712*
[43] *Tsinghua University, Beijing 100084, China*
[44] *Valparaiso University, Valparaiso, Indiana 46383*
[45] *Variable Energy Cyclotron Centre, Kolkata 700064, India*
[46] *Warsaw University of Technology, Warsaw, Poland*
[47] *University of Washington, Seattle, Washington 98195*
[48] *Wayne State University, Detroit, Michigan 48201*
[49] *Institute of Particle Physics, CCNU (HZNU), Wuhan 430079, China*
[50] *Yale University, New Haven, Connecticut 06520*
[51] *University of Zagreb, Zagreb, HR-10002, Croatia*

(Dated: October 4, 2007)

We report the first measurement of the opening angle distribution between pairs of jets produced in high-energy collisions of transversely polarized protons. The measurement probes (Sivers) correlations between the transverse spin orientation of a proton and the transverse momentum directions of its partons. With both beams polarized, the wide pseudorapidity ($-1 \leq \eta \leq +2$) coverage for jets permits separation of Sivers functions for the valence and sea regions. The resulting asymmetries are all consistent with zero and considerably smaller than Sivers effects observed in semi-inclusive

deep inelastic scattering (SIDIS). We discuss theoretical attempts to reconcile the new results with the sizable transverse spin effects seen in SIDIS and forward hadron production in pp collisions.

PACS numbers: 13.75.cs, 13.87.-a, 13.88.+e, 24.70.+s

Hard scattering of light quarks has little sensitivity to one quark's spin orientation transverse to the scattering plane, due to helicity conservation (chiral symmetry) in the limit of zero quark mass for both quantum chromodynamics (QCD) and electrodynamics. Nonetheless, sizable sensitivity to the transverse spin of a *proton* has been observed at high energies in both semi-inclusive deep inelastic scattering (SIDIS) of electrons [1] and proton-proton collision processes with cross sections well described by perturbative QCD (pQCD) [2]. Theoretical interpretations of these results [3] attribute them to a combination of soft QCD spin-dependent features of the proton wave function and of the final-state fragmentation of the struck quark into a hadron jet. Experiments that can unravel these contributions are essential to understand high-energy hadron spin dynamics.

Of particular interest, since it arises from orbital contributions to the proton spin [4], is the Sivers effect [5]: a correlation ($\langle \vec{s}_{\rm p} \cdot (\vec{p}_{\rm p} \times \vec{k}_T) \rangle \neq 0$) of initial-state parton transverse momentum ($\vec{k}_T$) with the proton's spin ($\vec{s}_{\rm p}$) and momentum ($\vec{p}_{\rm p}$). This three-vector correlation evades time-reversal violation when orbital components of the proton's light-cone wave function combine with initial (ISI) and/or final-state interaction (FSI) contributions to the scattering process [4, 6]. In the spirit of pQCD factorization of hadron cross sections, the Sivers effect involves parton distribution (Sivers) functions that depend on both $\vec{k}_T$ and longitudinal momentum fraction x_B. In contrast to ordinary factorization, gauge invariance demands that Sivers functions incorporate pQCD-calculable, but process-dependent, "gauge link factors" describing the partonic ISI/FSI. These lead to a predicted sign change between SIDIS and Drell-Yan processes [6, 7].

A non-zero Sivers effect revealed [8] in SIDIS pion production from a transversely polarized proton target can be fitted with Sivers functions of opposite sign and different magnitude for u vs. d quarks [3]. This account can be tested by treating within a common framework Sivers asymmetries measured for other pQCD processes, such as jet production in pp collisions [9]. For colliding proton beams moving along the $\pm\hat{z}$-axis and vertically ($\pm\hat{y}$) polarized, the Sivers effect gives a preferential sideways ($\pm\hat{x}$) kinematic boost to jet momenta, causing [10] a spin-dependent average deviation from 180° azimuthal opening angle between jets from a hard two-body parton scattering. We report the first measurement of this di-jet asymmetry, which probes gluon, as well as quark, Sivers functions. The data were taken in 2006 with $\sqrt{s} = 200$ GeV transversely polarized proton beams at the Relativistic Heavy-Ion Collider (RHIC), providing 1.1 pb^{-1} of luminosity integrated by the STAR detector [11].

Continuous operation of two Siberian snakes [12] in each RHIC ring guaranteed that the beam polarizations were vertical at STAR. The spin orientation alternated for each successive bunch of one beam and for each pair of bunches of the other. Four distinct alternation patterns were used for different beam stores to minimize false asymmetries from accidental correlations of beam properties with bunch number. Beam polarizations, monitored during each store by proton-carbon Coulomb-nuclear interference polarimeters [13], averaged 59% (57%) for the $+\hat{z}$ ($-\hat{z}$) beam for this analysis, with statistical uncertainties far smaller than the ±12% relative uncertainty in the (online) polarimeter calibration.

The detector subsystems critical to the present measurements are the barrel (BEMC) and endcap (EEMC) electromagnetic calorimeters [11], with full azimuthal (ϕ) coverage spanning pseudorapidities $|\eta| \leq 0.98$ and $1.08 \leq \eta \leq 2.0$, respectively. The EMC's are subdivided into towers that subtend small regions in $\Delta\eta$ and $\Delta\phi$. Tower gains are calibrated, to a precision $\approx \pm 5\%$ to date, with minimum-ionizing particles and electrons tracked with STAR's time projection chamber (TPC). Digitized tower signals are summed in STAR trigger hardware over $\Delta\eta \times \Delta\phi \approx 1.0 \times 1.0$ "jet patches". The hardware triggers used required: (1) a transverse energy sum $E_T > 4.0$ GeV for at least one BEMC or EEMC jet patch; (2) $E_T^{tot} > 14$ GeV summed over the full EMC; and (3) coincident signals indicating a valid collision from forward ($3.3 \leq |\eta| \leq 5.0$) beam-beam counters (BBC) at each end of the STAR detector [14]. A software (level 2) trigger then passed only that subset of events with at least two localized (to $\Delta\eta \times \Delta\phi = 0.6 \times 0.6$) EMC energy depositions, with $E_{T1(2)} \geq 3.6$ (3.3) GeV and $|\phi_1 - \phi_2| \geq 60°$.

The trigger selectivity for di-jets is illustrated in Fig. 1(a-c) by EMC information from the level 2 processor. The azimuthal angles $\phi_{1,2}$ (referred to the horizontal $+\hat{x}$-axis in the STAR coordinate frame) and pseudorapidities $\eta_{1,2}$ (measured with respect to $+\hat{z}$) of the two jet axes are obtained from E_T-weighted centroids of the EMC tower locations in the level 2 jet clusters. The η values use an event vertex determined with coarse resolution ($\sigma_z \approx 30$ cm) from the time difference between the two BBC's. The correlation in Fig. 1(a) is dominated by intense di-jet ridges centered around $|\phi_1 - \phi_2| = 180°$.

Initial-state $\vec{k}_T$ is manifested in a given event by a tilt of the jet axes, characterized by the deviation $|\phi_1 - \phi_2| - 180°$ and the di-jet bisector angle ϕ_b. The Sivers analysis combines these features in a "signed" azimuthal opening angle ζ, chosen $> 180°$ when $\cos\phi_b > 0$ (implying $k_T^x > 0$) and $< 180°$ otherwise. STAR's left-right symmetric di-

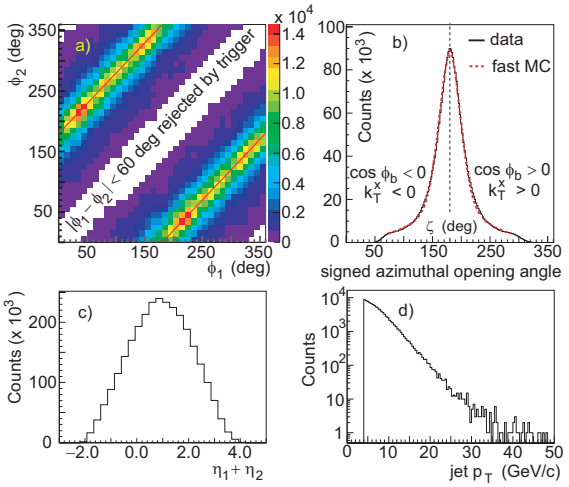

FIG. 1: Distributions of events that pass the STAR di-jet trigger with respect to (a) di-jet azimuthal angles, (b) signed azimuthal opening angle (ζ), and (c) pseudorapidity sum, all using EMC energies only. The p_T distribution (d) is from full jet reconstruction for 2% of all runs analyzed. The fit in (b) is from fast Monte-Carlo simulations described in the text.

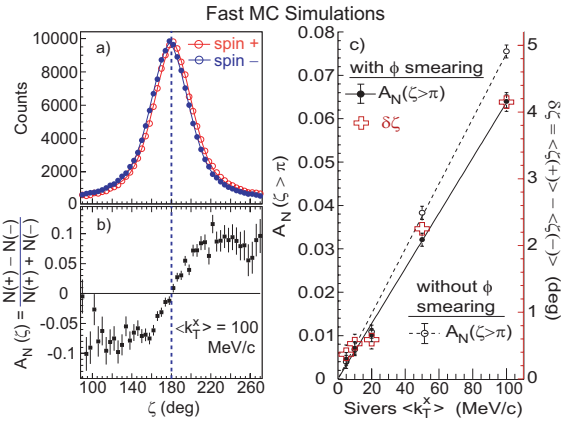

FIG. 2: Fast MC simulations of di-jet Sivers asymmetries: (a) the ζ spectra for two beam spins and (b) the resulting yield asymmetry *vs* ζ for an assumed spin-dependent centroid shift $\pm\langle k_T^x \rangle = \pm 100$ MeV/c. (c) The spin-dependent ζ centroid shift (right scale) and ζ -integrated analyzing power (left scale) *vs* assumed $\langle k_T^x \rangle$, including (solid line) and excluding (dashed) ϕ resolution smearing of the reconstructed jet.

jet acceptance, reflected in the ζ symmetry in Fig. 1(b), minimizes systematic errors in our Sivers asymmetries.

The ζ distribution shape is well reproduced by "fast" Monte-Carlo (MC) simulations discussed below. The peak width ($\sigma_\zeta \approx 20°$) is dominated by intrinsic k_T distributions of the scattering partons, with smaller ϕ resolution contributions from the use of EMC energy alone for partial jet reconstruction ($\sigma_\phi^{\rm EMC-full} = 3.9°$), and from deviations between parent parton directions and even fully reconstructed jet axes ($\sigma_\phi^{\rm full-parton} = 5.0°$). These resolutions were determined, respectively, from the data themselves and from simulations utilizing the PYTHIA 6.205 event generator [15] and GEANT [16] modeling of the detector response. In the first case we compared, for a small sample of runs, the ϕ, ζ and η values (the latter yielding $\sigma_\eta^{\rm EMC-full} = 0.07$) determined at trigger level and from full jet reconstruction including offline gain calibrations and TPC tracks. Full reconstruction, following the approach in [9], but with a jet cone radius of 0.6 and p_T threshold of 4.0 GeV, does not greatly improve the net parton directional resolution ($\sigma_\phi^{\rm EMC-parton} = 6.3°$). Thus, the trigger-level di-jet analysis reported here is sufficient to explore initial results and their implications for theoretical descriptions of the Sivers effect.

The transverse momentum (p_T) distribution from full jet reconstruction (Fig. 1(d)) indicates dominance of partons with $x_T \equiv 2p_T/\sqrt{s} \approx 0.05 - 0.10$. The actual x_B range probed is broad due to the η coverage in Fig. 1(c). In a leading-order parton-parton scattering interpretation, $\eta_1 + \eta_2 = \ln(x_B^{+z}/x_B^{-z})$. The range $2 < (\eta_1 + \eta_2) < 3$ is then primarily sensitive to $x_B^{+z} \approx 0.1 - 0.4$, $x_B^{-z} \approx 0.01 - 0.04$, so that the two beams provide complementary information on valence- and sea-dominated regions.

Fast MC simulations in Fig. 2 illustrate some Sivers asymmetry measures. Two-parton scattering events were generated with a uniform distribution in ϕ_1 (and $|\phi_2 - \phi_1| = 180°$) and a p_T distribution reproducing Fig. 1(d). Each parton was given a random initial-state $\vec{k}_T$ drawn from a model distribution centered about zero for the y-component, but about $\pm\langle k_T^x \rangle$ for the x-component in a polarized proton, with the sign correlated with $\vec{s}_{\rm p} \times \vec{p}_{\rm p}$ to simulate the Sivers effect. The sum $\vec{k}_T^{+z} + \vec{k}_T^{-z}$ was added to the initially thrown outgoing momenta to deduce boosted azimuthal angles that could then be further smeared with a Gaussian of $\sigma_\phi^{\rm EMC-parton} = 6.3°$.

For Figs. 1(b) and 2, the model k_T distribution combines a Gaussian peak with symmetric exponential tails enhancing larger $|k_T^{x,y}|$, as needed to reproduce the roughly flat ζ spectrum wings. Full event reconstruction shows these wings to be dominated by multi-jet events, reflecting higher-order pQCD processes, where only the two jets with highest EMC energy were analyzed at level 2. With ϕ smearing included, the k_T distribution fitted to Fig. 1(b) has an rms width $\langle (k_T^{x,y})^2 \rangle^{1/2} = 1.26$ GeV/c, consistent with the trend of earlier particle correlation results [17] from pp collisions. The linear relationship of single-spin observables to $\langle k_T^x \rangle$ seen in Fig. 2(c) is rather insensitive to details of the k_T distribution shape.

Figures 2(a,b) show that the primary Sivers manifestation is a spin-dependent ζ centroid shift, leading to a spin up *vs.* down yield asymmetry antisymmetric about $\zeta = 180°$, as predicted in [10]. We sort real data into statistically independent ζ distributions for the four beam spin combinations ++, etc., where the first (second) index is the sign of the $\hat{y}$ polarization component at STAR

for the $+\hat{z}$ ($-\hat{z}$) beam. To compare with predictions integrated over the k_T distributions, we extract analyzing powers $A_N^{\pm z}(\zeta > \pi)$ averaged over ζ and ϕ_b, by fitting asymmetries measured for individual $|\cos\phi_b|$ bins:

$$f P_{\pm z} |\cos\phi_b| A_N^{\pm z}(\zeta > \pi) = [r_{\pm z}(\phi_b) - 1]/[r_{\pm z}(\phi_b) + 1], \quad (1)$$

where the cross-ratios r exploit the antisymmetry in Fig. 2(b) by treating di-jet yields N_{ij} with spin-up and $\zeta > \pi$ as equivalent to spin-down, $\zeta < \pi$. For example:

$$r_{+z}(\phi_b) \equiv \sqrt{\frac{\sum N_{+j}(\zeta > \pi, \phi_b)}{\sum N_{-j}(\zeta > \pi, \phi_b)} \cdot \frac{\sum N_{-j}(\zeta < \pi, \phi_b)}{\sum N_{+j}(\zeta < \pi, \phi_b)}}, \quad (2)$$

where sums extend over $-\hat{z}$-beam spin states $j = +, -$. The cross-ratio eliminates the need for independent relative luminosities for different spin combinations and cancels several potential systematic errors. $(P_{\pm z})|\cos\phi_b|$ denotes beam polarization components normal to the di-jet bisector within each $|\cos\phi_b|$ bin. The factor $f = 0.85 \pm 0.07$ in Eq. 1 corrects for dilution of a parton-level asymmetry by ϕ resolution smearing (compare solid and dashed lines in Fig. 2(c)), with an uncertainty to allow for model-dependence in determining f from simulations. The equivalent of Eq. 2 for r_{-z} has yields $N_{i-}(\zeta > \pi)$ (summed over $+\hat{z}$-beam spin states i) in the numerator. This gives $A_N > 0$ when $\vec{k}_T$ points preferentially leftward for a spin-up beam, following the Madison [18], rather than the opposite Trento [19] convention used in [3].

The measured asymmetries, integrated over $|\zeta - \pi| \leq 68°$, are compared to calculations [20] in Fig. 3. The systematic error bands combine in quadrature the f uncertainty and the effect of multi-jet contributions to the ζ distribution wings. Limits on the latter effect are deduced by looking for variations in $r_{\pm z}$, beyond statistical fluctuations, when we extract yields alternatively by changing the ζ integration range or subtracting a constant baseline fitted to the ζ wings independently for each spin state. We neglect much smaller instrumental asymmetries from bunch-to-bunch variations in beam path or in azimuthally localized beam background.

The measured asymmetries are consistent with zero, and remain so for higher software EMC E_T thresholds. BBC yields analyzed with the same code reproduce the associated non-zero asymmetry [14] in both magnitude and sign. Our results are an order of magnitude smaller than π^+ SIDIS Sivers asymmetries [8], for predominant di-jet sensitivity (see Fig. 3(a-b)) to both high-x_B quarks ($A_N^{+z}(\eta_1 + \eta_2 \gtrsim 2)$) and low-$x_B$ gluons ($A_N^{-z}(\eta_1 + \eta_2 \gtrsim 2)$). The η-integrated sample (2.6×10^6 di-jet events) has mean $\langle A_N^{\pm z}(\zeta > \pi)\rangle = 0$ within statistical uncertainties $\approx \pm 0.002$, probing (see Fig. 2(c)) Sivers $\langle k_T^x \rangle$ preferences as small as $\sim \pm 3$ MeV/c, or $\pm 0.2\%$ of $\langle (k_T^{x,y})^2 \rangle^{1/2}$.

Recent theory breakthroughs [22, 23] and our preliminary results [24] have stimulated rapid evolution in treatments of transverse single-spin asymmetries (SSA). Bacchetta *et al.* [22] deduced the gauge link structure for hadron or jet production in pp collisions, where both ISI and FSI contribute, with opposite phases. Ji *et al.* [23] demonstrated strong overlap between Sivers effects and twist-3 quark-gluon correlations (QGC) [25]. The pQCD calculations [20] in Fig. 3 exploit these developments to incorporate cancellations that were absent or less severe in predictions [3] made before the measurements. The calculations use one set of unpolarized distribution functions, yielding the parton contribution fractions in Fig. 3(a-b), but three different models of u- and d-quark Sivers functions in Figs. 3(c-f). All assume zero gluon Sivers function. They are integrated over a p_T range (5–10 GeV/c) well matched to our data, and further over the STAR η acceptance [20]. We have reversed the sign of the calculated A_N to apply the Madison convention.

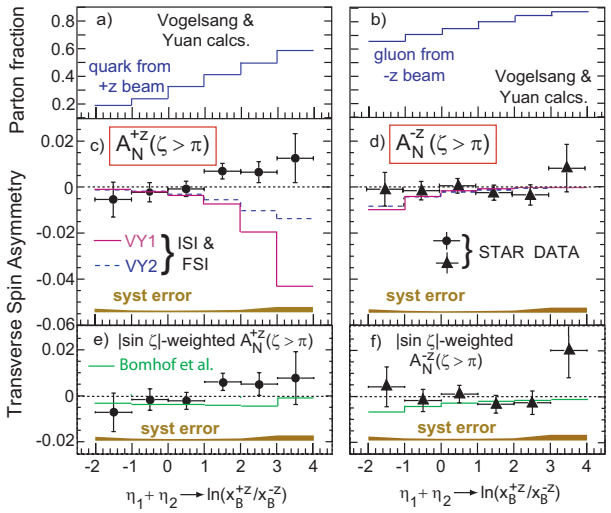

FIG. 3: Measured and calculated asymmetries vs. di-jet pseudorapidity sum for $+\hat{z}$ (left) and $-\hat{z}$ (right) beams. (a,b): Fraction of the calculated di-jet cross section with a quark (gluon) from the $+\hat{z}$ ($-\hat{z}$) beam. (c,d): Unweighted asymmetries compared with pQCD calculations [20] (histograms) for two models of quark Sivers functions fitted to SIDIS results [8]. (e,f): Asymmetries for $|\sin\zeta|$-weighted yields, compared with calculations [20, 21] based on twist-3 quark-gluon correlations. Vertical (horizontal) bars on the data indicate statistical uncertainties (bin widths). The systematic error bands exclude a $\pm 12\%$ beam polarization normalization uncertainty.

The calculations in Fig. 3(c-d) use [20] quark Sivers functions fitted [3] to SIDIS data [8] with the d-quark functional form tied either to $u(x_B)$ (VY1) or $d(x_B)$ (VY2) unpolarized distribution functions. For $\eta_1 + \eta_2 \gtrsim 2$ the A_N^{+z} predictions reflect the sizable HERMES asymmetries, diluted [20] by partial u *vs* d and ISI *vs* FSI (the latter were missing in [3]) cancellations, while $A_N^{-z} \approx 0$ because gluon Sivers effects are ignored.

Figure 3(e-f) compares A_N measured and calculated [20] with yields in Eq. (2) weighted by $|\sin\zeta|$ [21], as

needed to connect to a more robustly interpretable gauge link structure [22], given the apparent breakdown of factorization for back-to-back dijets [26]. The measurements, consistent with zero at all ζ, are hardly affected by the weighting, but the calculations sample a different Sivers function moment that can no longer be constrained by unweighted SIDIS asymmetries. Taking constraints instead from QGC fits [27] to A_N for inclusive forward hadron production in pp collisions [2, 28] gives di-jet A_N comparable in magnitude to our data, via more complete ISI vs. FSI and u vs. d cancellations [20]. The $u-d$ cancellation can be tested in the future by filtering quark flavors with the leading hadron's charge sign for each jet.

In summary, we report the first measured spin asymmetries for di-jet production in pp collisions. The analysis searches for a spin-dependent sideways tilt of the di-jet axes sensitive to Sivers correlations between the proton's transverse spin and transverse momentum preferences of its partons. All measured asymmetries are consistent with zero, whether dominated by partons in the valence or sea regions. Perturbative QCD calculations can reconcile these results with sizable SSA observed for forward hadron production in pp and for semi-inclusive deep inelastic scattering via cancelling contributions from u and d quarks and from initial- and final-state interactions. These data constrain unified theoretical accounts for transverse SSA in hard pQCD processes, and their connection to parton orbital momentum.

We thank the RHIC Operations Group and RCF at BNL, and the NERSC Center at LBNL for their support. This work was supported in part by the Offices of NP and HEP within the U.S. DOE Office of Science; the U.S. NSF; a sponsored research grant from Renaissance Technologies Corporation; the BMBF of Germany; CNRS/IN2P3, RA, RPL, and EMN of France; EPSRC of the United Kingdom; FAPESP of Brazil; the Russian Ministry of Science and Technology; the Ministry of Education and the NNSFC of China; IRP and GA of the Czech Republic, FOM of the Netherlands, DAE, DST, and CSIR of the Government of India; Swiss NSF; the Polish State Committee for Scientific Research; SRDA of Slovakia, and the Korea Sci. & Eng. Foundation.

[1] A. Airapetian *et al.* [HERMES Collaboration], Phys. Rev. Lett. **84**, 4047 (2000); Phys. Rev. **D 64**, 097101 (2001); and Phys. Rev. Lett. **94**, 012002 (2005).
[2] J. Adams *et al.* [STAR Collaboration], Phys. Rev. Lett. **92**, 171801 (2004).
[3] W. Vogelsang and F. Yuan, Phys. Rev. **D 72**, 054028 (2005), and references therein.
[4] S.J. Brodsky, D.S. Hwang and I. Schmidt, Phys. Lett. **B 530**, 99 (2002) and Nucl. Phys. **B 642**, 344 (2002).
[5] D.W. Sivers, Phys. Rev. **D 41**, 83 (1990) and Phys. Rev. **D 43**, 261 (1991).
[6] J.C. Collins, Phys. Lett. **B 536**, 43 (2002).
[7] D. Boer, P.J. Mulders and F. Pijlman, Nucl. Phys. **B 667**, 201 (2003); J.C. Collins and A. Metz, Phys. Rev. Lett. **93**, 252001 (2004).
[8] A. Airapetian *et al.* [HERMES Collaboration], Phys. Rev. Lett. **94**, 012002 (2005).
[9] B.I. Abelev *et al.* [STAR Collaboration], Phys. Rev. Lett. **97**, 252001 (2006).
[10] D. Boer and W. Vogelsang, Phys. Rev. **D 69**, 094025 (2004).
[11] K.H. Ackermann, *et al.* [STAR Collaboration], Nucl. Instrum. Meth. **A 499**, 624 (2003); M. Beddo *et al.*, *ibid.* 725; C.E. Allgower *et al.*, *ibid.* 740.
[12] I. Alekseev *et al.*, Nucl. Instrum. Meth. **A 499**, 392 (2003).
[13] O. Jinnouchi *et al.*, RHIC/CAD Accelerator Physics Note 171 (2004).
[14] J. Kiryluk [STAR Collaboration], *hep-ex*/0501072, published in Spin 2004 Conf. Proc., Trieste, Italy.
[15] T. Sjostrand *et al.*, Comput. Phys. Commun. **135**, 238 (2001).
[16] GEANT 3.21, CERN program library.
[17] S.S. Adler *et al.* [PHENIX Collaboration], Phys. Rev. **D 74**, 072002 (2006); T. Henry, Ph.D. Thesis, Texas A& M University (2006)(see Fig. 66).
[18] Proc. 3rd Intl. Symp. on Polarization Phenomena in Nuclear Physics, eds. H.H. Barschall and W. Haeberli (University of Wisconsin Press, Madison, 1971), p. xxv.
[19] A. Bacchetta, U. D'Alesio, M. Diehl and C.A. Miller, Phys. Rev. **D 70**, 117504 (2004).
[20] C.J. Bomhof, P.J. Mulders, W. Vogelsang and F. Yuan, Phys. Rev. **D 75**, 074019 (2007), and private communication.
[21] The $|\sin\zeta|$-weighted asymmetries from [20] are divided by the measured $\langle|\sin\zeta|\rangle = 0.33$ in Fig. 3(e,f). This rescaling corrects for a failure to weight the calculated unpolarized cross section, as needed to compare to measured analyzing powers with unit maximum magnitude.
[22] A. Bacchetta, C.J. Bomhof, P.J. Mulders and F. Pijlman, Phys. Rev. **D 72**, 034030 (2005).
[23] X. Ji, J.-W. Qiu, W. Vogelsang and F. Yuan, Phys. Rev. Lett. **97**, 082002 (2006), and references therein.
[24] J. Balewski [STAR Collaboration], *hep-ex*/0612036.
[25] J. Qiu and G. Sterman, Phys. Rev. **D 59**, 014004 (1998).
[26] J. Collins and J.-W. Qiu, Phys. Rev. **D 75**, 114014 (2007).
[27] C. Kouvaris, J.-W. Qiu, W. Vogelsang and F. Yuan, Phys. Rev. **D 74**, 114013 (2006).
[28] D.L. Adams *et al.* [FNAL-E704 Collaboration], Phys. Lett. **B 264**, 462 (1991); J.H. Lee [BRAHMS Collaboration], Proceedings of SPIN2006 Conference, AIP Conf. Proc. **915**, 533 (2007)